IOP Conference Series: Earth and Environmental Science

PAPER • OPEN ACCESS

Research on the deformation and failure evolution of sandstone under triaxial compression based on PFC^{2D}

To cite this article: X B Yang *et al* 2017 *IOP Conf. Ser.: Earth Environ. Sci.* **61** 012090

IOP Conf. Series: Earth and Environmental Science **61** (2017) 012090 doi:10.1088/1755-1315/61/1/012090

Research on the deformation and failure evolution of sandstone under triaxial compression based on PFC^{2D}

X B Yang, X X Han, T B Zhou and E L Liu

School of Resource and Safety Engineering, China University of Mining and Technology (Beijing), Beijing 100083, China
hanxxyydy123@126.com

Abstract: Through the comparative analysis of the results of the triaxial compression experiments of sandstone and the numerical simulation results of particle flow code PFC^{2D} under the same conditions, the typical simulation curve and the corresponding simulation process were selected to analyze the evolution characteristics of the surface deformation field, the evolution characteristics of the velocity field and displacement field of the deformation localization bands of sandstone under triaxial compression. Research results show that the changes of the velocities and displacements of deformation localization bands corresponds to the change of stress during compression; In the same deformation localization band, the dislocation velocities are always in the same direction, but in the direction vertical to the localization band, the localization band sometimes squeezes and sometimes stretches; At different positions of the same deformation localization band, the dislocation velocities and extrusion velocities are both different at the same time; In the post-peak stage of loading, along the same deformation localization band, the dislocation displacements close to both loaded ends are generally greater than the ones near to the middle position of the specimen, the stretching displacements close to both loaded ends are generally smaller than the ones near to the middle position of the specimen.

1. Introduction

Rock is an important and complicated medium material in engineering and its deformation and failure are closely related to various rock geological disasters, so the research of deformation and failure about rock has always been a matter of great concern in the academic and engineering circles [1] and has important scientific and engineering significances [2, 3]. Due to the existence of many cracks and various micro defects in the rock material, damage and localized centralized development of micro cracks will occur under external forces leading to the local deformation and failure of rock [4]. So in most cases, the deformation and failure of rock are triggered by the development of deformation localization [5-9] and it is very important to study the evolution process of deformation localization.

The deformation localization of rock is closely related to the stress state of rock. In the aspect of relationship between the evolution of deformation localization and mechanical properties of loading, Zhang [4] used digital laser speckle method to study the process of the deformation localization of two kinds of soft rocks including mud sandstone and mudstone under uniaxial compression and gained the change laws of local deformation failure of soft rocks under different stress conditions. Song et al. [5, 10] took white light digital speckle correlation method as the mean of experimental observation, studied the deformation evolution of whole loading process and the displacement evolution of deformation concentration areas of rock through uniaxial compression experiments and obtained related evolution laws. Hao and Sun [8] observed synchronously the surface displacement field of rock samples and the load-displacement curve under uniaxial loading through the white light speckle synchronous measurement system which was self built and analyzed the evolution characteristics of surface deformation field. These research results have positive significances for understanding the local deformation evolution of rock under uniaxial compression. However, due to the limitations of the experimental conditions at present, the relationship between the local deformation evolution and the loading stress in the whole process of triaxial compression is rarely reported. Although it is difficult to explore it through experiments, the numerical simulation method provides a new way.

As a powerful discrete element numerical simulation software, PFC^{2D} can better simulate the experimental process of rock under triaxial compression [11, 12]. So this paper simulated the whole process of the triaxial compression of sandstone based on PFC^{2D} and selected a typical simulation curve and the corresponding simulation process to study the evolution characteristics of the surface deformation field, the evolution characteristics of the velocity field and displacement field of the deformation localization bands about sandstone under triaxial compression through the comparative analysis of experimental results and numerical simulation results.

2. Experimental and numerical simulation results of the triaxial compression of sandstone under different confining pressures

Electro hydraulic servo testing machine of RLJW-2000 type for the triaxial compression of rock was used to conduct the triaxial compression tests of sandstone samples under the constant confining pressures of 5MPa, 10MPa, 20MPa, 30MPa respectively. Controlled axial strain rate was used in these experiments and the axial strain rate of triaxial compression tests was 0.005mm/s. Based on laboratory experiments, particle flow code PFC^{2D} was used to simulate the whole process of the triaxial compression of sandstone under corresponding different confining pressures. In the simulation, the particles were produced by radius expansion method and the simulation was carried out by parallel bond model. To be the same as the loading mode and loading rate of experiments, the simulation processes were also loaded by controlling axial strain, in which, axial compression was conducted by controlling the speed of the upper and lower walls. While the speed of side walls was controlled by the numerical servo system to maintain a constant confining pressure. The contrast curves of stress-strain between experiments and numerical simulation under different confining pressures were shown in figure1.

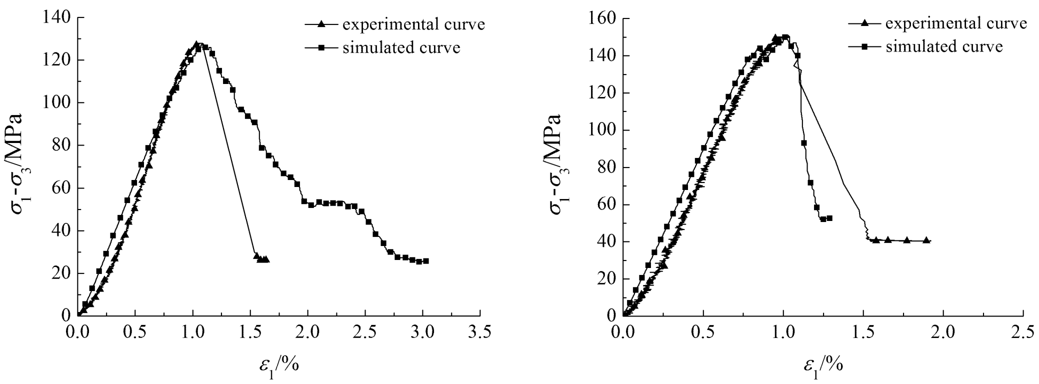

(a)Confining pressure of 5MPa (b) Confining pressure of 10MPa

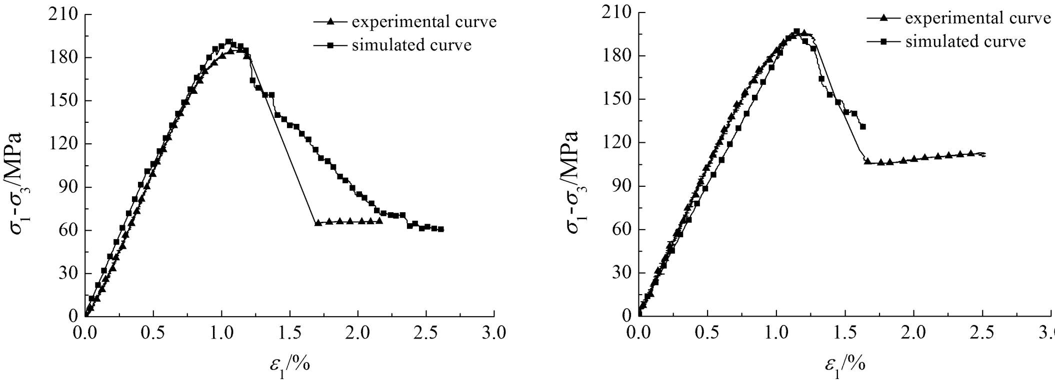

(c) Confining pressure of 20MPa (d)Confining pressure of 30MPa

Figure 1. Contrast curves of stress-strain between experiments and simulation under triaxial compression with different confining pressures

As shown in figure 1, under different confining pressures, the stress-strain curves of sandstone in triaxial compression experiments are close to the numerical simulation curves, the triaxial compressive strength between experiments and simulation are basically the same and the final failure form (as shown in figure 3(j)) is shear failure, which is consistent with the actual form of experimental destruction, so the particle flow code PFC^{2D} can be used to simulate the mechanical properties of rock more realistically. Therefore this paper studied the evolution characteristics of the surface deformation field, the evolution characteristics of the velocity field and displacement field of the deformation localization bands of sandstone during deformation and failure under triaxial compression based on the numerical simulation of PFC^{2D}.

3. Analysis of the evolution characteristics of deformation field

The simulated compression process under the confining pressure of 20MPa was selected to study the evolution laws of the deformation field of sandstone during deformation failure. The stress-strain curve was shown in figure 2 and ten typical identification points were selected on the curve. Then the corresponding failure figures of the specimen about every identification point were shown in figure 3. In figure 3, when cracks occured among particles, the particles would show different colors which indicated bonds among particles had been broken. The particles with the same color indicated that they were well bonded.

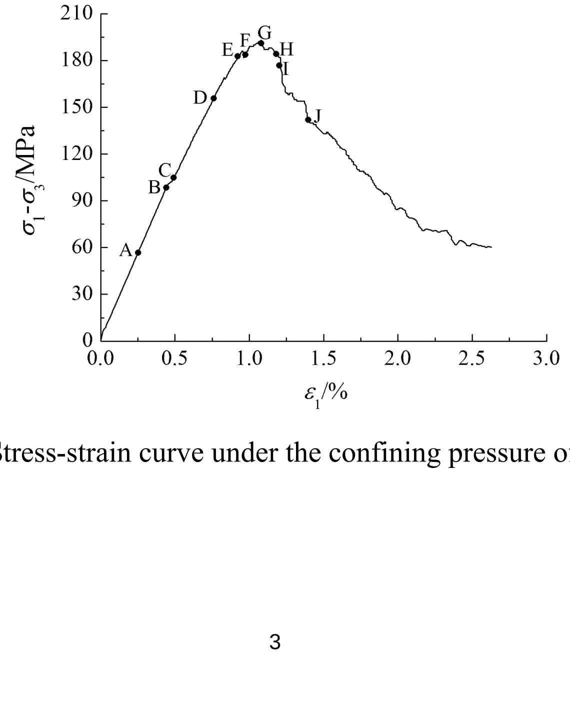

Figure 2. Stress-strain curve under the confining pressure of 20MPa

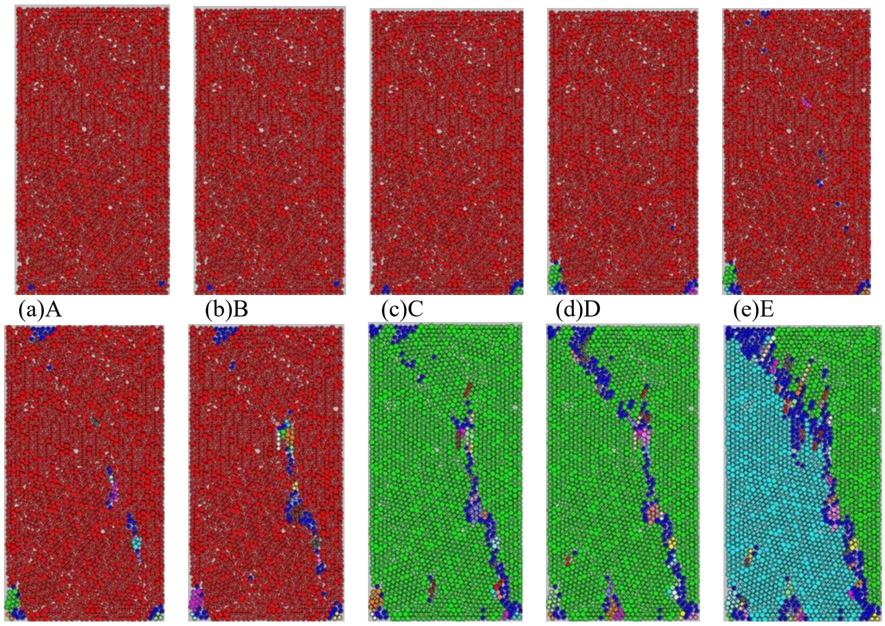

Figure 3. Failure figures about different identification points

From figure 2 and figure 3, the identification points A, B, C and D are located in the linear elastic stage. At this stage, the deformation of the specimen is homogeneous. Because of the occurrence of micro damage at the bottom of the specimen, a turn from point B to point C appears on the stress-strain curve. As a result, the stress-strain curve of the specimen don't extend along the original straight line. But due to the extension of cracks at the bottom boundary is slow, the stress-strain curve continues to rise. The identification points E and F are located in the plastic stage, and inhomogeneous deformation occurs. At point E, cracks have appeared in parts of the specimen. As the stress continues to increase, the intersection and penetration of cracks appears in local areas at point F. And at the peak stress of point G, this phenomenon is more obvious. Identification points H, I and J are located in the stage of strain softening, and at this stage, the cracks in the specimen continue to extend, converge and perforate, leading to the final failure of the specimen which is shown at point J. At point J, the colors of left and right part are different, indicating that the bonds between two parts are broken completely, forming shear slip bands.

4. Analysis of the evolution characteristics of velocity field in deformation localization bands

In the whole process of rock loading, the velocity and displacement evolution of deformation localization bands are closely related to the stress situation of the specimen. Therefore, it is necessary to study the evolution characteristics of the velocity and displacement of deformation localization bands. Figure 4 is the identification figure of deformation localization bands, in which the deformation localization bands were identified as M, N and the localization bands M and N divided the surface of specimen into two regions: P and Q. In order to explore the formation of deformation localization bands M and N, four sets of symmetry points vertical to localization bands were selected on both sides of the localization bands M and N, namely the points 1-8 in figure 4, in which the distance from each point to the localization band was equal. For the accuracy and reliability of the quantitative study, the velocity values of 7 particles were taken at each point, and the average value was taken as the speed at the point. The horizontal velocities and vertical velocities of each set of symmetry points were decomposed respectively along the orientation parallel and vertical to deformation localization bands, and the differences of the corresponding velocity components between symmetric points were solved as the dislocation velocity and extrusion velocity of this position in the deformation localization bands. In this paper, the dislocation velocities in a clockwise direction along the deformation localization bands were regarded as positive, and the extrusion velocities vertical to the deformation localization bands were considered positive. Through processing, the change curves of velocities between different symmetry points were shown in figure 5.

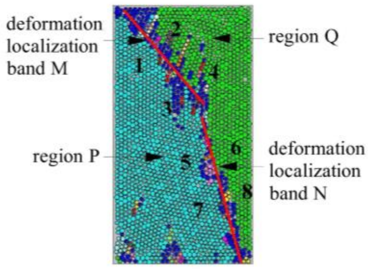

Figure 4. Identification figure of deformation localization bands

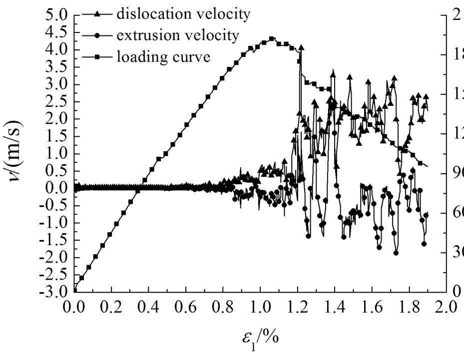

(a)Velocity variation of point 1 relative to point 2

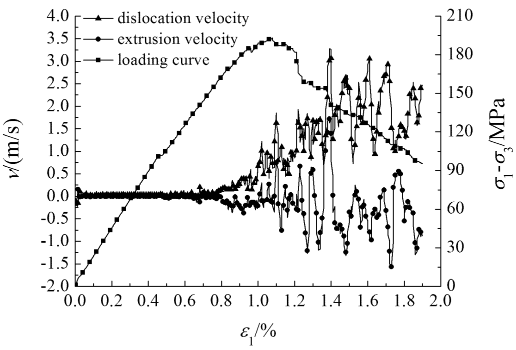

(b)Velocity variation of point 3 relative to point 4

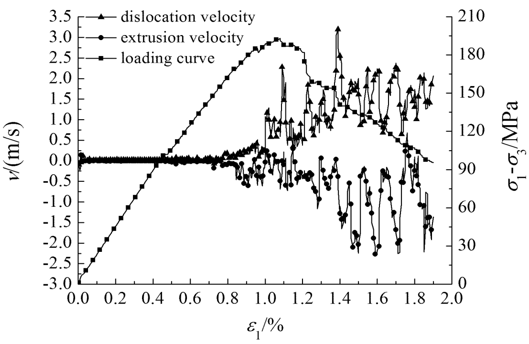

(c)Velocity variation of point 5 relative to point 6

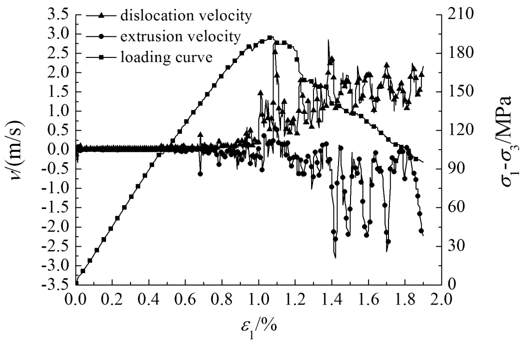

(d)Velocity variation of point 7 relative to point 8

Figure 5. Change curves of velocities between different symmetrical points

As shown in figure 5, in the linear elastic stage of stress-strain curve, the dislocation velocities and extrusion velocities between symmetric points of each group are basically zero. In the plastic stage and the post-peak stage, speed gradually present serrated fluctuations. The fluctuation amplitude of the velocities in the plastic stage is small, which indicates that the cracks are slowly expanding. In the whole process of stress loading, the region P and region Q have been moving along the clockwise direction of deformation localization bands. However, the dislocation velocities have not always been increasing, but repeatedly alternating between increase and decrease. In the direction vertical to localization bands, the region P and the region Q sometimes squeeze and sometimes stretch, and the velocities also repeatedly alternate between increase and decrease. But after the cracks are fully connected, the region P and the region Q will show tensile state basically. In figure 5, by comparing figure (a), (b), (c) and (d), a conclusion can be gained that at different positions of the same deformation localization band, the velocities are different at the same time, which indicates the expansion rates of cracks are different along the deformation localization band, cracks appear successively and cracks expansion have directionality.

5. Analysis of the evolution characteristics of displacement field in deformation localization bands

The analysis method of the evolution characteristics of displacement field in deformation localization bands is the same as the one of velocity field. The horizontal displacements and vertical displacements of each symmetry points were still decomposed respectively along the orientation parallel and vertical to deformation localization bands, and the differences of the corresponding displacement components between symmetric points were solved as the dislocation displacement and extrusion displacement of this position in the deformation localization bands. The dislocation displacements in a clockwise direction along the deformation localization bands were still regarded as positive, and the extrusion displacements vertical to the localization bands were also considered positive. Through processing, the evolution curves of the dislocation and extrusion displacements of the symmetry points on both sides of deformation localization bands were shown in figure 6 and figure 7 respectively.

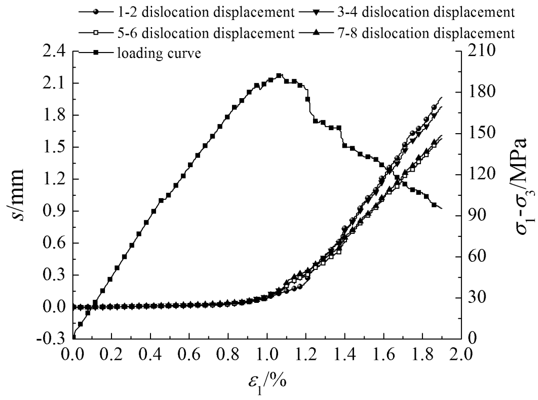

Figure 6. Evolution curves of the dislocation displacements of symmetrical points

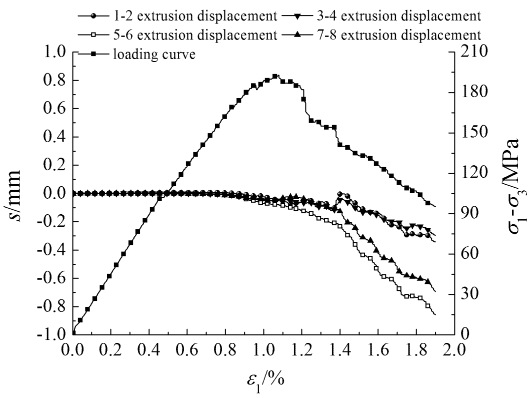

Figure 7. Evolution curves of the extrusion displacements of symmetrical points

As shown in figure 6, in the pre-peak stage of stress, the region P and region Q move along the clockwise direction of the deformation localization bands. The dislocation displacements of the symmetric points in each group exhibit linear evolution in the elastic stage, and starts to transite to the nonlinear evolution in the plastic stage. Because of the expansion, intersection and perforation of the cracks before the peak point, and the occurrence of dislocation displacements at the same time, the bearing capacity of the specimen begins to decrease. After the peak point of stress, the dislocation displacements of deformation localization bands increase gradually. And due to the sliding instability of the weak surfaces after peak point, the dislocation displacements increase sharply after the complete rupture between region P and region Q. At different positions of the same deformation localization band, the differences of dislocation displacements are not big. In figure 6, for deformation localization band M, the dislocation displacement between point 1 and point 2 is slightly larger than the one between point 3 and point 4. And for deformation localization band N, the dislocation displacement between point 5 and point 6 is slightly smaller than the one between point 7 and point 8.

In figure 7, region P produces a slight stretching in the direction vertical to the deformation localization bands relative to region Q in the pre-peak stage of stress and the stretching displacements also evolve from the linear evolution of elastic stage to the nonlinear evolution of plastic stage. In the post-peak stage, the stretching displacements of deformation localization bands increase gradually. Like dislocation displacements, the stretching displacements increase sharply after the complete rupture between region P and region Q. In the post-peak stage, the stretching displacements at different positions of the same deformation localization band are different. In figure 7, the stretching displacement between point 1 and point 2 differs little from the one between point 3 and point 4 in the deformation localization band M, but the stretching displacement between point 5 and point 6 is obviously larger than the one between point 7 and point 8 in the deformation localization band N.

Through the comprehensive analysis of figure 6 and figure 7, a conclusion can be obtained that in the post-peak stage of rock loading, along the same deformation localization band, the dislocation displacements close to both loaded ends are generally greater than the ones near to the middle position of the specimen, the stretching displacements close to both loaded ends are generally smaller than the ones near to the middle position of the specimen. However, due to the randomness of damage evolution, abnormal phenomena may occur. In figure 7, for example, the stretching displacement between point 1 and point 2 is first smaller and then slightly larger than the stretching displacement between point 3 and point 4 in the post-peak stage.

6. conclusions

The triaxial compression experiments of sandstone under different confining pressures were carried out firstly, and then based on the experiments, numerical simulation was conducted by using PFC^{2D} under the same conditions. Through the comparative analysis of experimental results and numerical simulation results, a typical simulation curve and the corresponding simulation process were selected to study the evolution characteristics of the surface deformation field, the evolution characteristics of the velocity field and displacement field of deformation localization bands about sandstone under triaxial compression and the following conclusions were obtained.

(1) Through the selection of the typical identification points on the stress-strain curve and the comparative analysis with the damage images of corresponding points, the forming process of the deformation localization bands are obtained.

(2) The dislocation velocities and extrusion velocities of deformation localization bands are basically zero in the elastic stage, they have small fluctuations in the plastic stage and have larger fluctuations in the post-peak stage. In the same deformation localization band, the dislocation velocities are always in the same direction, but in the direction vertical to the localization band, the localization band sometimes squeezes and sometimes stretches. And at different positions of the same deformation localization band, the dislocation velocities and extrusion velocities are varied at the same time.

(3) The dislocation displacements and extrusion displacements of deformation localization bands exhibit linear evolution in the elastic stage, and starts to transite to the nonlinear evolution in the plastic stage. In the post-peak stage, the dislocation displacements and extrusion displacements continue to increase, and the values of both displacements increase sharply after the localization bands are completely penetrated.

(4) In the post-peak stage of rock loading, along the same deformation localization band, the dislocation displacements close to both loaded ends are generally greater than the ones near to the middle position of the specimen, the stretching displacements close to both loaded ends are generally smaller than the ones near to the middle position of the specimen.

Acknowledgements

The authors are grateful to Natural Science Foundation of China (No. 50904071, 51274207) for the financial support to this work.

References

[1] Zhao Z H and Xie H P 2008 *JOURNAL OF SICHUAN UNIVERSITY (ENGINEERING SCIENCE EDITION)* **40** 26–31
[2] Bieniawski Z T, Denkhaus H G and Vogler U W 1969 *International Journal of Rock Mechanics and Mining Sciences and Geomechanics Abstracts* **6** 323–41
[3] Pan Y S 1999 *Study on Rockburst Initiation and Failure Propagation* (Beijing: Tsinghua University)

[4] Zhang D M 2004 *Theoretical and experimental research on deformation localization and instability of rock* (Chongqing: Chongqing University)
[5] Song Y M, Ma S P, Yang X B and Wang X 2011 *Chinese Journal of Rock Mechanics and Engineering* **30** 170–75
[6] Mogi K 1968 *Bulletin of the Earthquake Research Institute Tokyo Imperial University* **46** 1103–25
[7] Wu L X, Liu S J, Wu Y H and Wu H P 2002 *International Journal of Rock Mechanics and Mining Sciences* **39** 825–31
[8] Hao S W and Sun J 2008 *JOURNAL OF EXPERIMENTAL MECHANICS* **23** 89–95
[9] Wong T F, Baud P and Klein E 2001 *Geophys. Res. Lett.* **28** 2521–24
[10] Song Y M, Jiang Y D, Ma S P, Yang X B and Zhao T B 2012 *Rock and Soil Mechanics* **33** 1352–56
[11] Yao T, Ren W, Que K S and Wang Y D 2012 *Soil Engineering and Foundation* **26** 70–73
[12] Yin C 2014 *Particle DEM Simulation for rock tests of direct tension and compression* (Chengdu: Southwest Jiaotong University)